DUAL POROSITY MODELS OF NEAR-WELL BEHAVIOUR OF A DISCHARGING WELL

Jaime Jemuel C. Austria, Jr.[1], and Michael J. O' Sullivan[2]

[1]Energy Development Corporation, Energy Center, 38/F One Corporate Centre Building,

Julia Vargas corner Meralco Avenue, Ortigas Center, Pasig City1605, Philippines

[2]Department of Engineering Science, University of Auckland, Auckland 1142 New Zealand

austria.jjc@energy.com.ph;m.osullivan@auckland.ac.nz

Keywords: *Geothermal reservoir, numerical simulation, dual- or double-porosity model, MINC*

ABSTRACT

The presence of fractures in a reservoir may significantly affect the behaviour of a discharging well and complicate the interpretation of drawdown/build-up well tests. Here simple radial models, in both single- and dual-porosity form, are used to investigate the near-well behaviour during a drawdown/build-up well test. The dual-porosity model is implemented with the multiple interacting continua or MINC system (Pruess and Narasimhan, 1982; Pruess and Narasimhan, 1985). For the dual-porosity model, the effect on near-well behaviour of important parameters such as fracture volume fraction, matrix permeability and fracture spacing is evaluated. The results are compared with those for a uniform porous (single-porosity) model.

1. INTRODUCTION

Most models of geothermal reservoirs have been based on an equivalent porous medium or single-porosity approach while a few have used the dual-porosity or MINC approach (Pruess and Narasimhan, 1985). In the single-porosity approach, fractured rock is represented as an equivalent, single continuum, possibly non-uniform and anisotropic.

Although single-porosity models are satisfactory for matching natural-state temperature and pressure data and long-term production histories of geothermal reservoirs, in some cases, the existence of fractures in the reservoir may affect the short-term production behaviour and the effect of injection on production (O'Sullivan et al., 2001).

Only a few geothermal fields have been modelled using the dual-porosity and MINC approach, mainly because the computational task involved for a standard three dimensional geothermal reservoir model is formidable and increases significantly for a dual-porosity model. Also the data available on fracture parameters are scarce (Bodvarsson et al., 1987).

By using a MINC model and the reservoir simulator MULKOM (Pruess, 1983), Bodvarsson and Witherspoon (1985) found for the Geysers in USA that the long-term pressure decline in steam wells is primarily controlled by the effective matrix permeability and fracture spacing as well as the initial liquid saturation and well spacing.

Kiryukhin et al. (2008) used a dual-porosity model of Pauzhetsky, Russia, and the inverse modelling software iTOUGH2 (Finsterle, 2004) to estimate reservoir parameters including fracture permeability and fracture porosity. In the Northwest Geysers in the USA, a MINC model was used to represent the shallow reservoir of the Coldwater Creek steamfield (Antúnez et al., 1994). In the numerical modelling of Ngatamariki in New Zealand, a dual-porosity MINC model was used as it was thought to be appropriate for assessing the effects of reinjection on production. The separate treatment of the fracture and matrix using the MINC method provided better estimates of thermal breakthrough (Clearwater et al., 2012).

Simulators other than TOUGH2 have also been used to set up dual-porosity models of geothermal systems. For example, in the case of the Rotokawa geothermal field in New Zealand, a dual-porosity model was set up using TETRAD (Bowyer and Holt, 2010). For Cerro Prieto, Mexico, Butler et al. (2000) developed a 3D dual-porosity model also using the TETRAD simulator. They used the model to optimize field management and plan capacity expansion. The grid blocks were divided into matrix and fracture blocks for seven layers in the model. The permeability of the fractures was set to be 100 times larger than the matrix permeability.

Yeltekin et al. (2002) developed a 3D dual-porosity model of Kizildere, Turkey, using the STAR simulator and modelled the effects of reinjection. Permeability values inferred from build-up tests and log-derived porosities were used in the model. For Mori, Japan, Osada et al. (2010) developed a dual-porosity 3D model also using the STAR simulator. The dual-porosity model enabled them to improve the match to production data in highly permeable areas and to analyse and predict the behaviour of the reservoir, production wells and reinjection wells. The natural state modelling was carried out with a single-porosity model while history matching and future prediction were carried out with a dual-porosity model.

Nakanishi et al. (1995) developed a MINC model of the Oguni geothermal reservoir (Japan), using a multi-phase reservoir simulator called SING. They used the model to assess the effect of cold water injection on the production sector.

The current research is part of a general study aimed at determining when dual-porosity models should be preferred ahead of single-porosity models. Here the limited problem of modelling a drawdown/build-up test is considered and the different types of behaviour predicted by dual-porosity models and single-porosity models are investigated. Parameters such as fracture and matrix permeability, fracture spacing and fracture volume fraction are investigated to check what difference these properties make on the near-well behaviour of a discharging well. The simulations are carried out using AuTOUGH2 (O'Sullivan, 2000), The University of Auckland's version of TOUGH2 (Pruess, 1991).

2. FRACTURE EFFECTS ON WELL DISCHARGE

The presence of fractures in a reservoir changes the results for a drawdown/build-up test significantly compared to those for a uniform reservoir and complicates the interpretation of the well tests. This was shown by numerical experiments conducted by O'Sullivan (1987a) on modelling well tests including constant rate drawdown followed by build-up for an initially two-phase and an initially liquid reservoir which flashes during the test (O'Sullivan, 1987b). O'Sullivan (1987b) used numerical modelling to estimate reservoir permeability and porosity by matching the production rate, discharge enthalpy and downhole pressure measured over a few days or weeks.

To investigate the effect of fractures in more detail, the work of O'Sullivan (1987b) is extended here by representing the presence of fractures by a multiple interacting continua or MINC model.

2.1 The MINC model

Pruess and Narasimhan (1982) were the first to provide an explanation for the production of dry-stream from an all-liquid geothermal system and devised the MINC method for treating the problem. The MINC method is a generalization of the dual-porosity model (Barenblatt et al., 1960; Warren and Root, 1963) which mathematically idealizes the flow region as two interacting media, namely, the fractures and the matrix.

The MINC method differs from the original dual-porosity approach by subdividing the matrix blocks further by using a nested sequence of blocks (Narasimhan, 1982) as shown in Figure 1. Thus the MINC method is able to accurately represent transient fracture-matrix flow in fractured porous media (Lai, 1986) and is able to provide a better numerical approximation for transient fracture-matrix interactions than a single-porosity model (Wu and Harasaki, 2009).

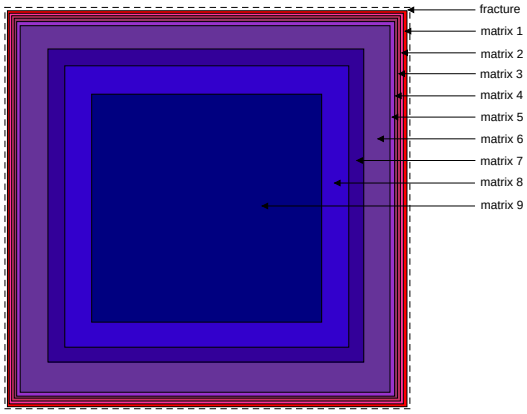

Figure 1: Nested volumes used in the MINC method, modified after Pruess et al. (2010)

A similar study by Pritchett (2005) showed that dual porosity models are required for simulating the high-enthalpy, and sometimes steam-dominated, discharge of wells in reservoirs with liquid-hydrostatic vertical profiles as such behaviour is related to high local heterogeneity in the reservoir with a sharp permeability contrast between a relatively impermeable rock matrix and fracture zones that penetrate the matrix and provide channels for fluid flow.

As the first stage of the present study, a model with parameters similar to the MINC model used by Pruess and Narasimhan (1982, 1985) was created. The aim was to use a finer grid than Pruess and Narasimhan to obtain more accurate results. Model parameters are listed in Table 1.

Table 1. Parameters for the model used by Pruess and Narasimhan

	Fracture	Matrix
Layer thickness	100m	100m
Permeability	26.8E-15m^2	1.0E-15m^2, 1.0E-16m^2, 1.0E-17m^2
Porosity	99%	8%
Rock grain density	2400kg/m^3	2400kg/m^3
Rock specific heat	960J/kg K	960J/kg K
Rock conductivity	4W/m K	4W/m K
Relative permeability	Corey: S_{lr}=0.30, S_{vr}=0.05	
Wellbore radius	0.1m	
Production rate	1.0kg/s	
Initial conditions	Pressure =35.268bar, Gas saturation =0.30 Temperature = 243°C	

As shown in Figure 2, the results obtained (dashed lines) are in good agreement with those obtained by Pruess and Narasimhan (1982, 1985).

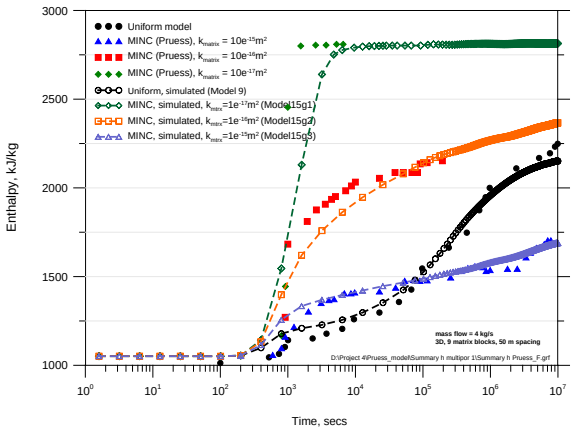

Figure 2: Simulated enthalpy transients, compared to the results from Pruess and Narasimhan (1982 , 1985)

2.1.1 Methodology

Using as basis the work of Pruess and Narasimhan (1982, 1985), a 1D radial model was set-up to look into the effects of varying matrix permeability and other fracture parameters such as fracture volume fraction and fracture spacing. The original model set up by Pruess and Narasimhan included a very large well block as an approximate method for representing a large skin effect. For the current study it was decided not to include any skin effect in order to be able to clearly distinguish differences between results from dual porosity models and those from a single porosity model. The parameters that were investigated are:

- Volume fraction of fractures (1E-2,1E-3,1E-4,1E-5)
- Matrix permeability (1mD, 0.1mD, 0.03mD, 0.01mD)
- Fracture spacing (20m, 50m)
- Number of matrix blocks (16, 13, 10, 8, 7, 5)

2.1.2 MINC model grid

The grid created for the MINC model is based on the grid for the uniform porous medium, as shown in Figure 3. The model has a thickness of 100 m and a total radius of 5 km.

The outer radius of the grid is chosen large enough so that no changes in the outer blocks are observed in any of the simulations.

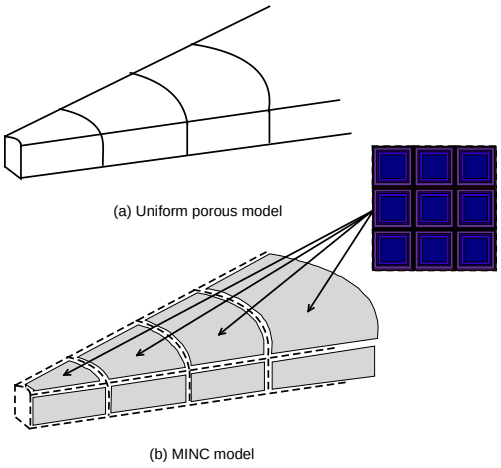

Figure 3: Block layout for the radial models

The mesh for the MINC model is set up using the pre-processor GMINC (Pruess, 2010). It creates the secondary mesh for the embedded matrix blocks which are required to accurately represent flow from the fracture into the rock matrix.

The first volume fraction is assigned to correspond to the fracture while the rest of the volume is assigned to the matrix. The volume fractions are chosen so as to provide good resolution for the flow in the matrix.

Two sets of models using: *(a)* a fine matrix grid and *(b)* a coarse matrix grid, were created to check what difference the matrix grid resolution makes on the results. Each grid block of the main mesh is partitioned into a sequence of interacting continua according to an average fracture spacing of 20 m or 50 m and a nest of 16, 13, 10 or 8 matrix blocks in each reservoir block for the fine model and 10, 8, 7 or 5 matrix blocks in each reservoir block for the coarse model. The nest of matrix blocks is embedded in a fracture block with the whole system occupying the same space as the reservoir block in the uniform reservoir model. In all cases the first matrix block is assigned the same volume as the fracture and then the volume of successive matrix blocks is increased by an approximately constant factor. Thus as the volume fraction for the fractures is increased the number of blocks used in the matrix is decreased. (See Table 2.)

Table 2: MINC blocks and fracture volume fractions

Number of MINC blocks		Volume fraction, V_f
Fine model	Coarse model	
16	10	1E-5
13	8	1E-4
10	7	1E-3
8	5	1E-2

The fine MINC models are created by increasing the volume fractions using a factor of ~2.25 and the coarse MINC models are created by increasing the volume fractions using a factor of ~4. The fracture volume fraction is set to be 10^{-5}, 10^{-4}, 10^{-3} or 10^{-2}. The fracture network is assumed to be three-dimensional and thus the option THRED is used in GMINC.

2.1.3 Parameters for the MINC model

The single-porosity model is assigned a permeability of 50 millidarcy (mD). In the MINC model, the permeability of 50 mD is retained as the fracture permeability while the matrix is assigned a permeability of 1.0, 0.1, 0.03 or 0.01 mD. For each volume fraction of fractures, V_f, the porosity of the fracture is set very high, por_{frac}=0.99, and a matrix porosity is chosen such that effective porosity of the dual porosity model (see equation below) is the same as the porosity of the single porosity model.

$$por_{eff} = por_{frac} V_f + por_{mtrx}(1 - V_f)$$

Porosity values of 4.99905×10^{-2}, 4.9905×10^{-2}, 4.90492×10^{-2} and 4.040505×10^{-2} are used for fracture volume fractions of 1E-2, 1E-3, 1E-4 and 1E-5, respectively.

The Corey-type relative permeability function with residual immobile liquid and gas saturation values of 0.3 and 0.05 is used. The initial conditions for the model are a temperature of 243°C and a gas saturation of 0.3.

A production rate is chosen low enough, at 1 kg/s, so that the simulation can be completed even for very low values of matrix permeability.

The numerical simulations are carried out with an increasing time step sequence and are run to an end time of 1E+6 seconds. The rock and reservoir parameters used in the model are summarized in Table 3.

Table 3: Parameters for the MINC model

	Fracture	**Matrix**
Layer thickness	100m	100m
Permeability	50E-15m^2	1.0E-15m^2, 1.0E-16m^2 3.0E-17m^2, 1.0E-17m^2
Porosity	99%	4 to 4.9%
Rock grain density	2600kg/m^3	2600kg/m^3
Rock specific heat	1000J/kg K	1000J/kg K
Rock conductivity	2.5W/m K	2.5W/m K
Relative permeability	Corey: S_{lr}=0.30, S_{vr}=0.05	
Wellbore radius	0.11m	
Production rate	1.0kg/s	
Initial conditions	Pressure =35.268bar, Gas saturation =0.30 Temperature = 243°C	

2.1.4 Drawdown test using the MINC model

The drawdown stage of the test was simulated for the various cases and the production enthalpy and pressure in the well block were recorded. It was of particular interest to determine which model parameters gave the development of a high production enthalpy in a short time frame.

Variation of fracture volume fraction

The model behaviour is very sensitive to the fracture volume fraction (V_f). The highest, dry steam, production enthalpy (2802 kJ/kg) is attained when the fracture volume fraction is very small, within the range 1×10^{-4} to 1×10^{-5}, as seen in Figures 4 and 6 for the fine model and Figures 5 and 7 for the coarse model. As the fracture volume fraction increases, to $V_f = 1 \times 10^{-3}$, the maximum flowing enthalpy attained becomes lower, in this case 2090 kJ/kg for the fine model as seen in Figure 8 and 2063 kJ/kg for the coarse model as seen in Figure 9. For the highest value of V_f = 1x

10^{-2}, the dual porosity model gives a lower production enthalpy than the single-porosity model: 1398 kJ/kg for the fine model as seen in Figure 10 and 1385 kJ/kg for the coarse model as seen in Figure 11.

For V_f = 1x 10^{-2} or 1x10^{-3}, the production enthalpy is continuing to rise at the end of the simulation period whereas for the smaller values of V_f the enthalpy stabilises earlier. Experimentation with longer simulation periods show that even for the larger values of V_f the enthalpy eventually rises to a stable value. (See Figure 12 for example.)

Some similar results on the sensitivity of the behaviour of a MINC model to the fracture volume fraction were obtained in a modelling study of the Ogiri geothermal system in Japan. The MINC method was applied to selected grid blocks in a model of the shallow zone of the Ogiri geothermal system in Japan where a steam-water two-phase zone and the fractured Ginyu Fault is situated (Itoi et al., 2010; Kumamoto et al., 2009). The simulated enthalpies of the Ogiri reservoir obtained using the MINC model are consistently higher than those from the single porosity model but they do not match the production history (Kumamoto et al., 2009). Our results indicate that the fracture volume fraction of 2 x10^{-2} used in the Ogiri model may not be small enough.

Variations in matrix permeability

The model behaviour is also sensitive to the matrix permeability. Four values of matrix permeability were used, namely: 1mD, 0.1mD, 0.03mD, and 0.01mD. In all cases the fracture permeability is 50mD and the fracture spacing is 50m.

The flowing enthalpy increases when the matrix permeability becomes small compared to the fracture permeability. The increase in flowing enthalpy with decreasing matrix permeability is shown in Figures 4 to 11. The maximum flowing enthalpy is obtained most quickly when k_{mtrx} = 1E-17m^2 (0.01mD).

Low values of matrix permeability were used during production history-matching with the MINC model of Coldwater Creek steamfield in the Northwest Geysers in the USA where a few wells gave enthalpies in the range 2880 kJ/kg for the main reservoir and up to 3070 kJ/kg for the high-temperature zone. In the MINC model of Coldwater Creek, the estimated fracture transmissivites ranged from 0.5x10^{-10} to 1×10^{-10} m^3 (or 50 and 100 Darcy-m) while field-wide matrix permeabilities were very low ranging from 1x10^{-20} to 3×10^{-18} m^2, or 0.01 to 3μD (Antúnez et al., 1994).

Variations in the number of matrix blocks

Fine and coarse models, using the same fracture volume fraction, were set-up to determine what difference the number of matrix blocks makes. By comparing Figures 4 and 5 for V_f = 1x 10^{-5} and Figures 6 and 7 for V_f = 1x 10^{-4}, Figures 8 and 9 for V_f = 1x 10^{-3}, and Figures 10 and 11 for V_f = 1x 10^{-2}, it is observed that there is no noticeable difference between the enthalpy transients as a result of grid refinement. This lack of sensitivity to grid resolution is very encouraging because this means fewer MINC blocks may be used to attain the same enthalpy transients. However, the coarse grid is still quite fine and models with fewer matrix blocks should be investigated. Using fewer MINC elements will lessen the computational time considerably.

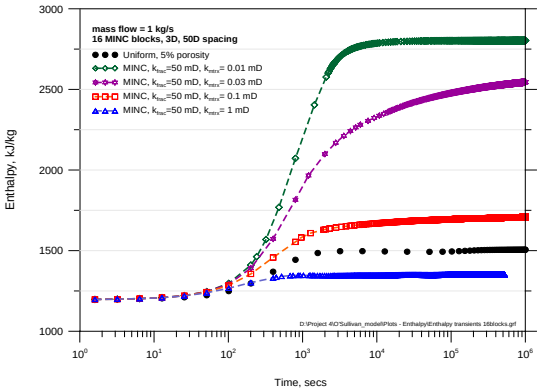

Figure 4: Enthalpy transients, fine grid, V_f = 1x 10^{-5}

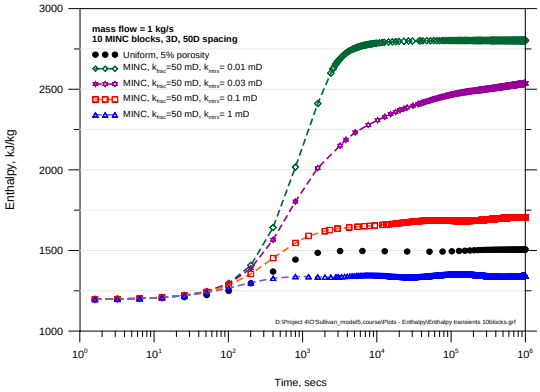

Figure 5: Enthalpy transients, coarse grid, V_f = 1x 10^{-5}

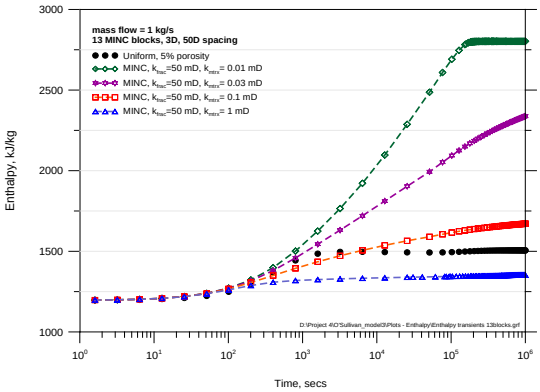

Figure 6: Enthalpy transients, fine grid, V_f = 1x 10^{-4}

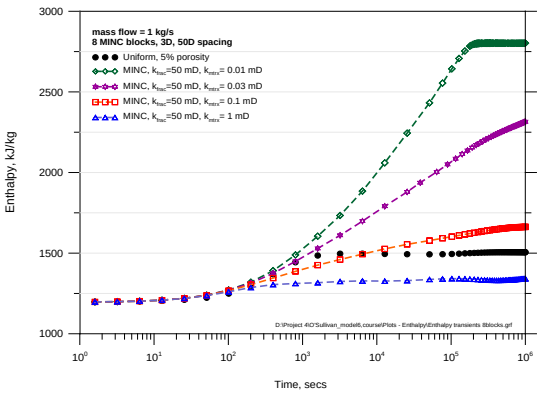

Figure 7: Enthalpy transients, coarse grid, V_f = 1x 10^{-4}

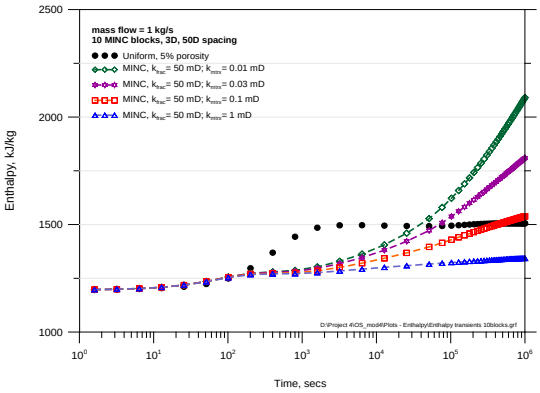

Figure 8: Enthalpy transients, fine grid, V_f = 1x 10^{-3}

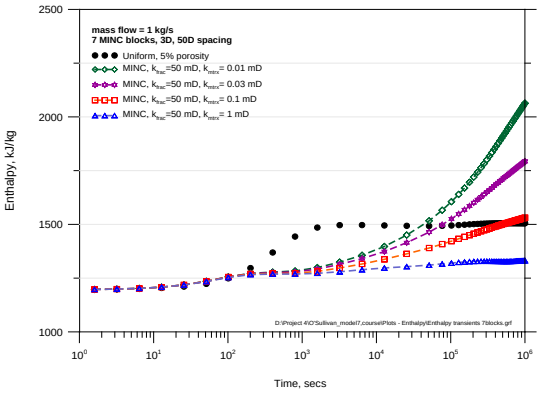

Figure 9: Enthalpy transients, coarse grid, V_f = 1x 10^{-3}

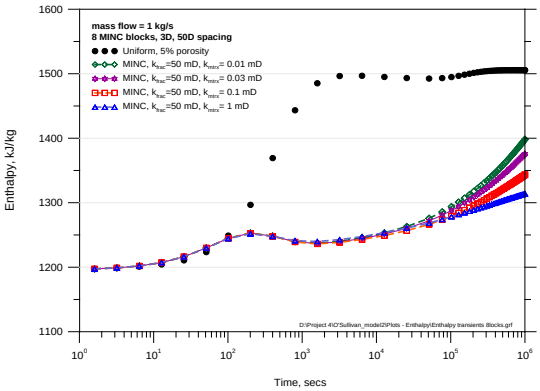

Figure 10: Enthalpy transients, fine grid, V_f = 1x 10^{-2}

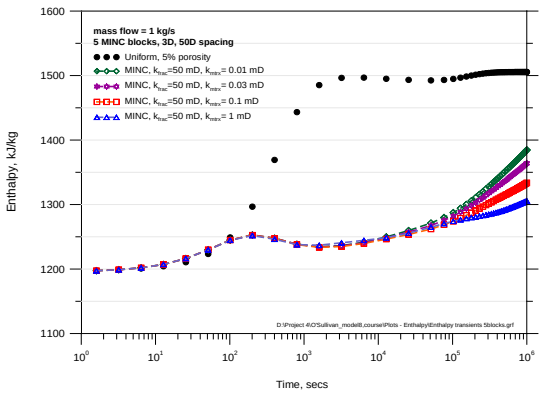

Figure 11:Enthalpy transients, coarse grid, V_f = 1x 10^{-2}

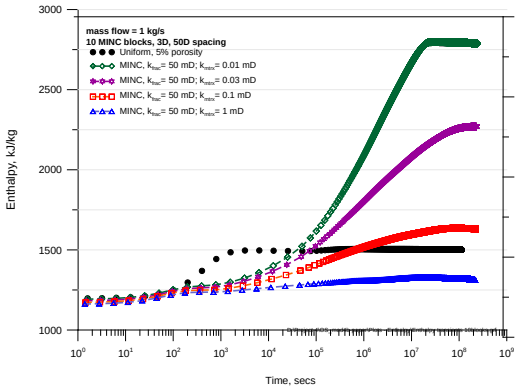

Figure 12: Enthalpy transients, fine grid, V_f = 1x 10^{-2}, longer production period

Variations in fracture spacing

The partitioning of matrix blocks based on distance from fractures leads to a pattern of nested volume elements (Pruess and Narasimhan, 1985). For any reservoir subdomain V_o, a "proximity function" PROX(x) can be defined which represents a total fraction of matrix volume within a distance x from the fracture interface (Pruess, 2010). In the MINC models used, a THRED proximity function is used which represents three sets of plane parallel infinite fractures at right angles with specified matrix block dimension. In the plots shown above a fracture spacing of 50m was used. The simulations were then repeated using a fracture spacing of 20m.

With the larger fracture spacing the flowing enthalpy rises more slowly but reaches the same stable enthalpy value. This behaviour is shown for V_f = 1x10^{-5} in Figure 13.

The effect of fracture spacing on the resulting enthalpy transients is more pronounced when the volume fraction of the fractures is larger and a stable enthalpy is not reached during the simulation period. A 464 kJ/kg difference in flowing enthalpy is observed between results of fracture distances of 20m (in colour) and 50m (in grey) for the fine model where V_f = 1x10^{-3}, as shown in Figure 14.

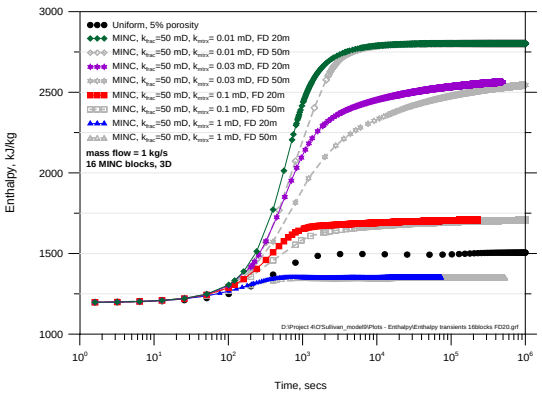

Figure 13: Enthalpy transients, fine grid, V_f = 1x 10^{-5}, fracture spacing 20 and 50m

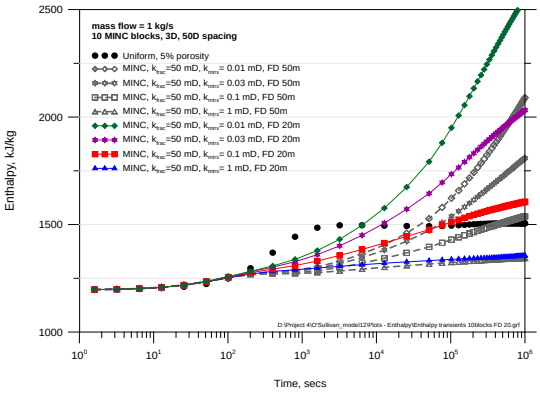

Figure 14: Enthalpy transients, fine grid, V_f = 1x 10^{-3}, fracture spacing 20 and 50m

In fractured media, changes in thermodynamic conditions due to boiling propagate rapidly in the fracture network and move slowly in the surrounding rock matrix. This behaviour is illustrated in the plots of vapour saturation against radial distance shown below in Figures 15 to 18. These plots help to explain why the enthalpy transients behave as shown above.

The plots of vapour saturation against radial distance show that higher vapour saturations of greater radial extent are obtained when the surrounding matrix permeability is low. For reference, the matrix starts from the outer volume (next to the fracture), which is designated as MINC level 2, and ends at the inner volume, which is designated as MINC level 16, for the 16 MINC block model.

The plot of radial vapour saturation for the 16-block fine model (V_f = 1x 10^{-5}) with a matrix permeability of 1mD is shown in Figure 15. Similar plots for other values of matrix permeability are shown in Figures 16 to 18. The sequence of plots clearly shows the increase in vapour saturation in the fracture as the matrix permeability decreases.

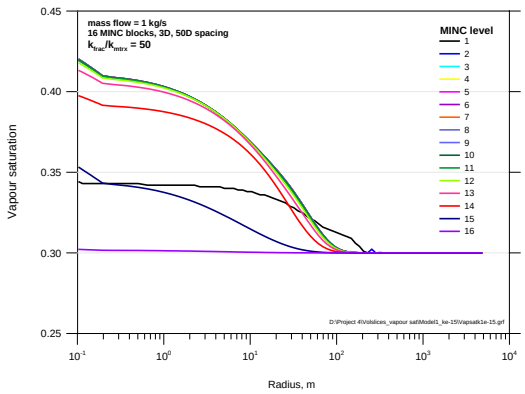

Figure 15: Vapour saturation vs. radius, fine model, V_f = 1x 10^{-5}, k_{mtrx} = 1mD

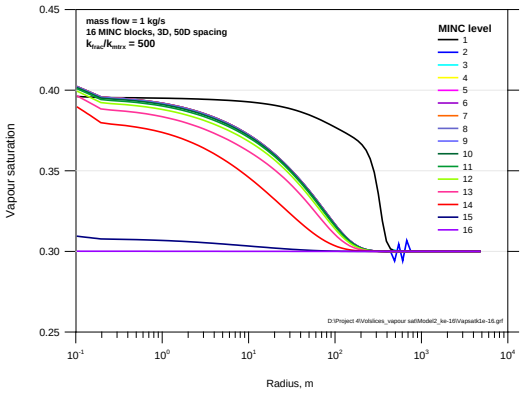

Figure 16: Vapour saturation vs. radius, fine model, V_f = 1x 10^{-5}, k_{mtrx} = 0.1mD

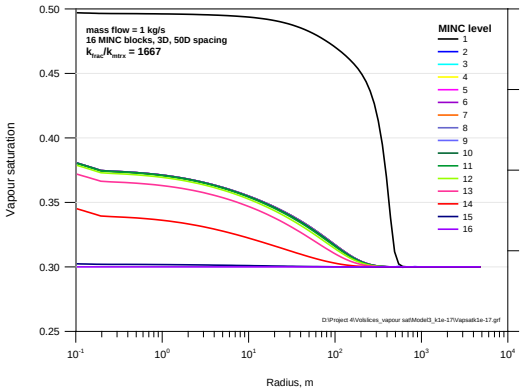

Figure 17: Vapour saturation vs. radius, fine model, V_f = 1x 10^{-5}, k_{mtrx} = 0.03mD

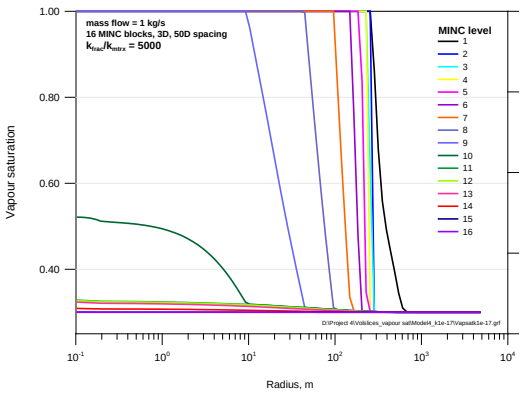

Figure 18: Vapour saturation vs. radius, fine model, V_f = 1x 10^{-5}, k_{mtrx} = 0.01mD

3. BUILD-UP TEST USING MINC MODEL

For the build-up test, the well is produced for 1e^6 seconds and then the well is shut for the same time period.

The dual-porosity behaviour of the MINC models is characterized by two parallel semilog straight lines and an S-shaped transition between them, as seen in Figure 19.

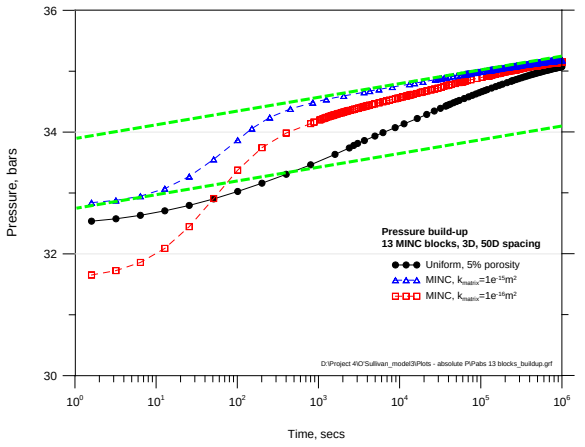

Figure 19: Buildup test, fine model, V_f = 1x 10^{-5}, various values of matrix permeability, semilog plot of pressure vs. log time

Plots of vapour saturation against radial distance for a 16-block MINC model (V_f = 1x 10^{-5}) at various values of matrix permeability are shown in Figures 20 to 23. The vapour saturation increases steadily from the inner volume (MINC level 16) to the outer volume (MINC level 1). The vapour saturation changes very slowly in the surrounding matrix but increases rapidly in the fracture network.

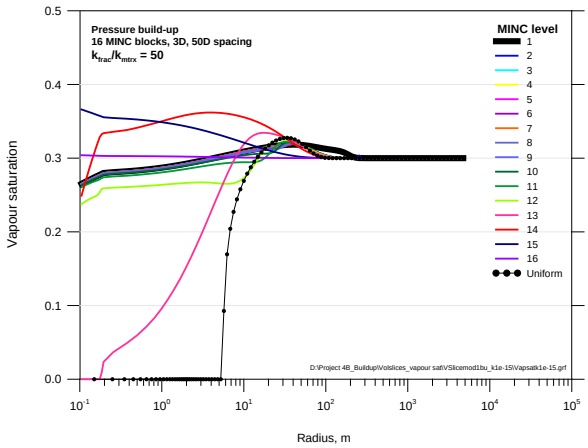

Figure 20: Buildup test, vapour saturation vs. radius, V_f = 1x 10^{-5}, fine model, k_{mtrx} = 1mD

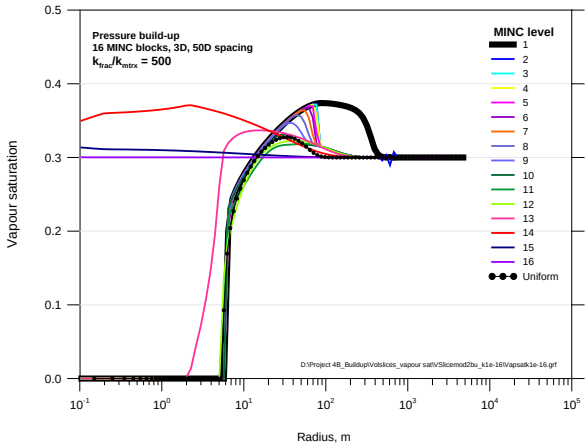

Figure 21: Buildup test, vapour saturation vs. radius, V_f = 1x 10^{-5}, fine model, k_{mtrx} = 0.1mD

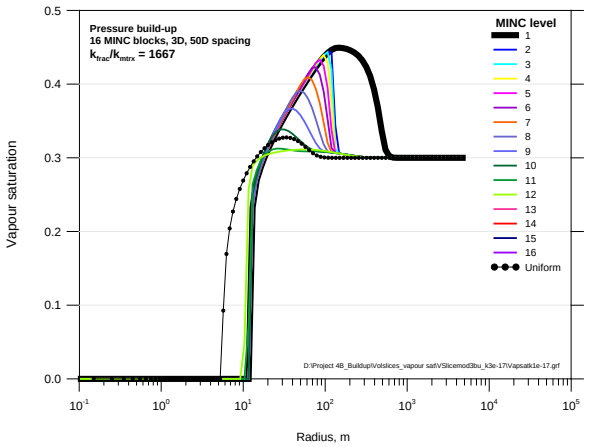

Figure 22: Buildup test, vapour saturation vs. radius, V_f = 1x 10^{-5}, fine model, k_{mtrx} = 0.03mD

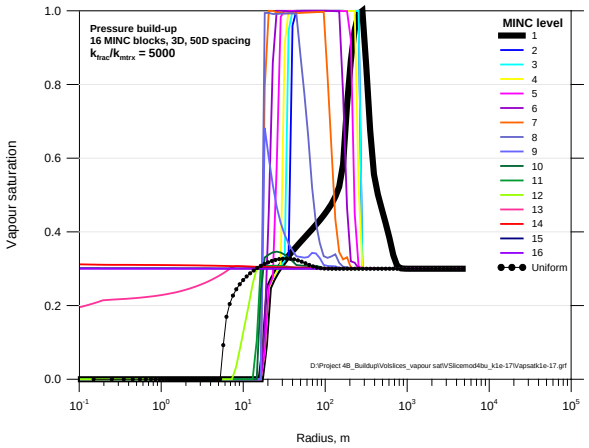

Figure 23: Buildup test, vapour saturation vs. radius, V_f = 1x 10^{-5}, fine model, k_{mtrx} = 0.01mD

4. SUMMARY AND CONCLUSIONS

The enthalpy transients for the production well show greatest sensitivity to the fracture volume fraction and matrix permeability. In cases where the volume fraction of fractures is small, a stable two-phase enthalpy is approached rapidly.

The highest, dry steam, enthalpy (2802 kJ/kg) is attained when the fracture volume fraction is very small, within the range 1x10^{-4} to 1x10^{-5}, for both fine and coarse models. As the fracture volume fraction becomes larger, the maximum flowing enthalpy attained gets lower for both the fine and coarse models. The model behaves somewhat differently when the fracture volume is large enough, e.g. when V_f = 1x 10^{-2}, as the enthalpy does not reach a stable value during the simulation period.

There is not much difference between the resulting enthalpy transients for the fine and coarse models which mean fewer MINC blocks could be used to attain the same results while decreasing the computational time.

A higher vapour saturation and greater radial extent of drying out is reached when the surrounding matrix permeability is lower. The changes in thermodynamic conditions due to boiling propagate rapidly in the fracture and move slowly in the surrounding rock matrix. The thermodynamic conditions vary rapidly in the matrix in the vicinity of the fracture.

REFERENCES

Antúnez, E.U., Bodvarsson, G.S. and Walters, M.A., 1994. Numerical simulation study of the Northwest Geysers geothermal field, a case study of the Coldwater Creek steamfield. Geothermics, 23(2): 127-141.

Barenblatt, G.I., Zheltov, I.P. and Kochina, I.N., 1960. Basic concepts in the theory of seepage of homogeneous liquids in fissured rocks. J. Appl. Math. Mech, 24(5): 1286-1303.

Bodvarsson, G.S., Pruess, K., Stefansson, V., Bjornsson, S. and Ojiambo, S.B., 1987. East Olkaria geothermal field, Kenya. 1. History match with production and pressure decline data. Journal of Geophysical Research, 92(B1): 521-539.

Bodvarsson, G.S. and Witherspoon, P.A., 1985. Flow rate decline of steam wells in fractured geothermal reservoirs, Lawrence Berkeley Lab., CA (USA).

Bowyer, D. and Holt, R., 2010. Case Study: Development of a Numerical Model by a Multi-Disciplinary Approach, Rotokawa Geothermal Field, New Zealand, World Geothermal Congress 2010, Bali, Indonesia.

Butler, S.J., Sanyal, S.K., Henneberger, R.C., Klein, C.W., Puente, H. and de Leon, J., 2000. Numerical Modeling of the Cerro Prieto Geothermal Field, Mexico. Transactions Geothermal Resources Council: 401-406.

Clearwater, J., Burnell, J. and Azwar, L., 2012. Modelling of the Ngatamariki Geothermal System, Thirty-Seventh Workshop on Geothermal Reservoir Engineering, Stanford University, Stanford, California.

Finsterle, S., 2004. Multiphase inverse modeling: Review and iTOUGH2 applications. Vadose Zone Journal, 3(3): 747.

Itoi, R., Kumamoto, Y., Tanaka, T., Takayama, J. and Department of Earth Resources Engineering, K.U., 2010. History Matching Simulation of the Ogiri Geothermal Field, Japan, Proceedings World Geothermal Congress 2010.

Kiryukhin, A.V., Asaulova, N.P. and Finsterle, S., 2008. Inverse modeling and forecasting for the exploitation of the Pauzhetsky geothermal field, Kamchatka, Russia. Geothermics, 37(5): 540-562.

Kumamoto, Y., Itoi, R., Tanaka, T. and Hazama, Y., 2009. Modeling And Numerical Analysis Of The Two-Phase Geothermal Reservoir At Ogiri, Kyushu, Japan.

Lai, C.H., Pruess, K., Bodvarsson, G.S., 1986. On the Accuracy of the MINC approximation. LBL-21025; Other: ON: DE86012753.

Nakanishi, S., Kawano, Y., Tokada, N., Akasaka, C., Yoshida, M. and Iwai, N., 1995. A reservoir simulation of the Oguni field, Japan, using MINC type fracture model, World Geothermal Congress pp. 1721-1726.

Narasimhan, T.N., 1982. Multidimensional numerical simulation of fluid flow in fractured porous media. Water Resources Research, 18(4): 1235-1247.

O'Sullivan, M.J., 1987a. Aspects of geothermal well test analysis in fractured reservoirs. Transport in Porous Media, 2(5): 497-517.

O'Sullivan, M.J., 1987b. Modelling of enthalpy transients for geothermal wells, Proceedings of the 9th New Zealand Geothermal Workshop, pp. 121-125.

O'Sullivan, M.J., 2000. AUTOUGH2 Notes. Geothermal Research Software., Department of Engineering Science, University of Auckland,.

O'Sullivan, M.J., Pruess, K. and Lippmann, M.J., 2001. State of the art of geothermal reservoir simulation. Geothermics, 30(4): 395-429.

Osada, K., Hanano, M., Sato, K., Kajiwara, T., Arai, F., Watanabe, M., Sasaki, S., Sako, O., Matsumoto, Y. and Yamazaki, S., 2010. Numerical Simulation Study of the Mori Geothermal Field, Japan.

Pruess, K., 1983. Development of the general purpose simulator MULKOM. Earth Sciences Division Annual Report 1982, Lawrence Berkeley Laboratory Report LBL-15500.

Pruess, K., 1991. TOUGH2: A general-purpose numerical simulator for multiphase nonisothermal flows, Lawrence Berkeley Lab., CA (United States).

Pruess, K., 2010. GMINC - A Mesh Generator for Flow Simulations in Fractured Reservoirs.

Pruess, K. and Narasimhan, T.N., 1982. On fluid reserves and the production of superheated steam from fractured, vapor-dominated geothermal reservoirs. Journal of Geophysical Research, 87(B11): 9329-9339.

Pruess, K. and Narasimhan, T.N., 1985. A Practical Method for Modeling Fluid and Heat Flow in Fractured Porous Media Society of Petroleum Engineers, Volume 25, Number 1.

Warren, J. and Root, P.J., 1963. The behavior of naturally fractured reservoirs. Old SPE Journal, 3(3): 245-255.

Wu, Y.S. and Harasaki, K., 2009. Conceptualization and Modeling of Flow and Transport Through Fault Zones.

Yeltekin, K., Parlaktuna, M. and Akin, S., 2002. Modeling of Kizildere geothermal reservoir, Turkey, pp. 1-8.